# Alteration of COX-1 and TLR4 expression in the mouse brain during chronic social defeat stress revealed by Positron Emission Tomography study

Motooka, Yumika ; Shinohara, Ryota ; Kitaoka, Shiho ; Uryu, Ai ; Li, Dongrui ; Neyama, Hiroyuki ; Cui, Yilong ; Kida, Tatsuya ; Arakaki,…

(Citation)
Journal of Pharmacological Sciences,157(3):156-166

(Issue Date)
2025-03

(Resource Type)
journal article

(Version)
Version of Record

Journal of Pharmacological Sciences 157 (2025) 156–166

Contents lists available at ScienceDirect

Journal of Pharmacological Sciences

journal homepage: www.elsevier.com/locate/jphs

Full paper

# Alteration of COX-1 and TLR4 expression in the mouse brain during chronic social defeat stress revealed by Positron Emission Tomography study

Yumika Motooka [a], Ryota Shinohara [a,**], Shiho Kitaoka [a,b], Ai Uryu [a], Dongrui Li [a], Hiroyuki Neyama [d], Yilong Cui [c,d,***], Tatsuya Kida [e], Wakiko Arakaki [e], Hisashi Doi [e,g], Yasuyoshi Watanabe [f,h], Tomoyuki Furuyashiki [a,*]

[a] Division of Pharmacology, Kobe University Graduate School of Medicine, Kobe, Japan
[b] Department of Pharmacology, School of Medicine, Hyogo Medical University, Nishinomiya, Japan
[c] Laboratory for Brain-Gut Homeostasis, School of Medicine, Hyogo Medical University, Nishinomiya, Japan
[d] Laboratory for Biofunction Dynamics Imaging, RIKEN Center for Biosystems Dynamics Research, Kobe, Japan
[e] Laboratory for Labeling Chemistry, And RIKEN Center for Biosystems Dynamics Research, Kobe, Japan
[f] Laboratory for Pathophysiological and Health Science, RIKEN Center for Biosystems Dynamics Research, Kobe, Japan
[g] Research Institute for Drug Discovery Science, Collaborative Creation Research Center, Organization for Research Promotion, Osaka Metropolitan University, Sakai, Osaka, Japan
[h] Department of Essential Healthcare Science, Kobe University Graduate School of Science, Technology and Innovation, Kobe, Japan

A B S T R A C T

Despite the recognized roles of neuroinflammation in mental illnesses, PET imaging on currently available biomarkers has limitations due to the lack of evidence demonstrating their relationship to the molecular and cellular events of inflammation associated with the pathology of mental illness. Rodent stress models, such as chronic social defeat stress (SDS), have identified crucial roles for COX-1 and TLR4, which are innate immune molecules, in chronic SDS-induced neuroinflammation and its behavioral consequences. In this study, we performed COX-1 and TLR4 PET imaging at multiple time points during chronic SDS in mice. For COX-1 PET imaging, we used the COX-1 PET probe *(S)*-[$^{18}$F]KTP-Me. Subchronic SDS transiently increased uptake and slower washout in broad regions of the brain, including the cerebral cortex, hippocampus, striatum, and thalamus. For TLR4 PET imaging, we developed a new BBB-permeable PET probe, [$^{11}$C]**1**, which detected LPS-induced neuroinflammation. Washout of [$^{11}$C]**1** was facilitated in the cerebellum after subchronic and chronic SDS and in the pons-medulla after chronic SDS. Collectively, our findings suggest the potential usefulness of COX-1 and TLR4 PET imaging in visualizing and understanding time-dependent process of neuroinflammation in stress-related mental illnesses.

## 1. Introduction

Chronic stress caused by aversive and psychological stimuli induces emotional and cognitive disturbance and precipitates mental illnesses, such as depression and post-traumatic stress disorder (PTSD).[1,2] Rodent stress models, such as chronic social defeat stress (SDS), have demonstrated that chronic stress induces inflammation in the brain and body, such as microglial activation and myeloid cell mobilization, respectively, both of which are involved in behavioral disturbance.[3,4] Inflammation in the body may underlie physical dysfunctions, such as cardiovascular, gastrointestinal, and metabolic disorders, which are often comorbid with depression.[5,6] Notably, stress-dysregulated bodily organs exacerbate behavioral disturbance via inflammation-related molecules.[3,7] Thus, the brain-body interaction through inflammation is pivotal for stress-induced behavioral disturbance.

Aligned with these findings in rodents, clinical studies have implicated inflammation in depression.[8] Proinflammatory cytokines and myeloid cells, such as neutrophils and monocytes, are increased in the peripheral blood of depressive patients.[3] Positron emission tomography (PET) imaging on 18 kDa translocator protein (TSPO), a mitochondrial transporter of cholesterol, has been used to suggest inflammation in the brains of depressive patients.[9–11] However, these current markers have limitations to understand and visualize inflammation in mental illnesses. Proinflammatory cytokines and myeloid cells in the peripheral blood cannot predict what organs are associated with inflammation. TSPO PET imaging does not necessarily reflect inflammation in the brain

* Corresponding author.
** Corresponding author.
*** Corresponding author. Laboratory for Brain-Gut Homeostasis, School of Medicine, Hyogo Medical University, Nishinomiya, Japan.
*E-mail addresses:* rshino@med.kobe-u.ac.jp (R. Shinohara), cuiyl@riken.jp (Y. Cui), tfuruya@med.kobe-u.ac.jp (T. Furuyashiki).

https://doi.org/10.1016/j.jphs.2025.01.006
Received 5 September 2024; Received in revised form 27 December 2024; Accepted 15 January 2025
Available online 16 January 2025

nor decipher the cellular mechanisms, since TSPO is involved in mitochondrial physiology and expressed in most of brain cells.[12,13] The development of PET imaging targeting the molecules that are enriched in inflammation-related cells and crucial for stress pathology may help overcome these shortcomings.

Rodent studies have identified the roles of innate immune molecules, such as prostaglandin (PG) $E_2$ and Toll-like receptor (TLR) 2 and 4 (TLR2/4) for stress-induced behavioral disturbance.[14,15] $PGE_2$ is a bioactive lipid mediator derived from arachidonic acid by sequential actions of cyclooxygenase (COX) and PGE synthase.[16] SDS increases brain $PGE_2$ synthesis via COX-1, which is selectively expressed in microglia, leading to behavioral disturbance via dopaminergic attenuation.[14] In addition, TLR2/4 mediate chronic SDS-induced microglial activation, leading to neuronal and behavioral disturbance via inflammation-related molecules including $PGE_2$.[15,17] Although their roles remain to be established in stress-induced inflammation in the body, COX-1 and TLR2/4 are essential in acute and chronic inflammation upon tissue damage and physical disorders.[18,19] Therefore, COX-1 and TLR2/4 may be attractive targets for PET imaging to visualize inflammatory responses in the brain and body for stress-related mental illnesses.

In this study, we used a PET probe for COX-1, $^{18}$F-labeled *(S)*-ketoprofen methyl ester,[20] to visualize COX-1 distribution in the body and brain during chronic SDS. In addition, we newly developed a brain-permeable $^{11}$C-labeled PET probe for TLR4, [$^{11}$C]**1**, to visualize TLR4 distribution in the brain during chronic SDS. Our findings showed distinct alterations in COX-1 and TLR4 PET activities in the body and brain at multiple timepoints during chronic SDS.

## 2. Materials and methods

### 2.1. Animals

Male C57BL/6N mice (7–8 weeks old), retired male ICR breeding mice, and male Sprague-Dawley rats weighing approximately 300 g were purchased from Japan SLC (Shizuoka, Japan) and maintained in our animal vivarium for at least one week before experiments. Animals were housed in a temperature- and humidity-controlled animal room with a 12-h light/dark cycle (light on between 8:00 and 20:00) with *ad libitum* access to feed and water. All animal care and experimental procedures were conducted in accordance with the Guide for the Care and Use of Laboratory Animals of the National Institute of Health Sciences and approved by the Animal Experimentation Committees of Kobe University and RIKEN.

### 2.2. Chronic social defeat stress

Chronic SDS was performed as previously described.[15,21] Male ICR mice were screened based on their aggressiveness to a male C57BL/6N mouse, as measured by attack latency and number in 3-min daily sessions over three days. ICR mice that showed an appropriate level of aggressiveness were used as aggressors. Experimental subjects, male C57BL/6N mice, were initially grouped in cages, housing 4–5 mice each. They were housed individually from one week before the first SDS session and throughout experiments. The mice were subjected to chronic SDS under 50-lux white light by transferring into a home cage of an aggressive ICR mouse for 10 min daily for 10 consecutive days. Different ICR mice were used on consecutive days. Experimental mice were returned to their home cage and left undisturbed until the next SDS or further examinations. As a control, C57BL/6N mice were handled similarly to mice with SDS but were put in an empty cage without SDS exposure.

### 2.3. Social interaction test

Social interaction test was performed as previously described.[15,21] To habituate to a test environment, an experimental mouse was placed into an open rectangular chamber (30 cm × 40 cm) containing an empty metal mesh cage (10 cm × 6 cm) at one end under a 10-lux red light illumination, and the mouse's locomotor activity was measured for 150 s. To measure the level of social interaction, an experimental mouse was returned into the same chamber for 150 s, but a novel male ICR mouse was enclosed within the metal mesh cage. The trajectory of mouse ambulation was video-recorded and analyzed using SMART video tracking software (PanLab Harvard Apparatus, Barcelona, Spain). A 30 cm × 9 cm rectangular zone opposite to the metal mesh cage was defined as the social avoidance zone. The proportions of the time spent in this zone were measured post hoc as an index of social avoidance.

### 2.4. Lipopolysaccharide-induced neuroinflammation

Under 1.5% isoflurane anesthesia, the head of each rat was fixed in a stereotaxic apparatus (Model 68,025, RWD Life Science, Shenzhen, China), and a small burr hole for lipopolysaccharide (LPS) microinjection was drilled in the skull above the right striatum (0.5 mm anterior and 3.2 mm lateral to the bregma). Then, LPS (strain 026:B6, Sigma-Aldrich) was diluted in saline to a concentration of 1 μg/μl and microinjected into the right striatum (4.5 mm ventral to the cortical surface) at a 0.2 μl/min rate using a UMP3 pump regulated by Micro-4 controller (World Precision Instruments, Sarasota, FL, USA).

### 2.5. Radiochemistry

$^{18}$F-Labeled *(S)*-ketoprofen methyl ester was synthesized as previously described.[20] Regarding specific ligands to TLR4, we focused on the sophisticated compound **1** with a pyrimidoindole structure, which was developed by the research groups of the University of California, San Diego.[22,23] They demonstrated that compound **1** is a selective agonist for TLR4 among several TLR isoforms, as shown by reporter cell assays.[22] This specificity was further confirmed by the observation that compound **1** induces inflammatory responses in bone marrow-derived dendritic cells at as low as 1 μM and in a manner dependent on TLR4 integrity. Structural analysis predicts a specific binding surface for compound **1** on the TLR4:MD2 complex. These characterizations have established compound **1** as a promising lead for developing TLR4 PET probes. According to their reports, methyl group at the N-5 position of pyrimidoindole structure was potentially crucial for not only increasing the agonistic activity to TLR4 but also decreasing cytotoxicity. For PET imaging, we investigated synthesis of $^{11}$C-labeled probe [$^{11}$C]**1** by incorporating radioactive [$^{11}$C]methyl group at the N-5 position. The radiolabeling was accomplished by the $^{11}$C-methylation using [$^{11}$C]methyl iodide and demethyl substrate **2**, the latter of which was prepared as the previous report.[22] Thus, by using a remote-controlled radiolabeling system to protect personnel from harmful radiation, demethyl substrate **2** (1.72 mg, 3.9 μmol) was reacted with [$^{11}$C]methyl iodide (radioactivity: ca. 40 GBq) in the presence of $Cs_2CO_3$ (2.6 mg, 8.0 μmol) at 90 °C for 4 min in dimethyl sulfoxide (DMSO, 400 μL). The reaction mixture was diluted with a mixed solution of acetonitrile (100 μL) and a 30 mM aqueous solution of ammonium acetate (100 μL), and then transferred to a reservoir vessel. After passing through a filter to remove solid substances, the mixture was injected into a semi-preparative HPLC system (Supplementary Fig. 1). The fraction of interest was collected in a flask, including sodium ascorbate to prevent radiolysis, and then concentrated under reduced pressure. After a formulation by sterilizing cartridges, [$^{11}$C]**1** was collected in a sterile vial using a mixed solution (3.0 ml) of saline, propylene glycol, and Tween 80 (volume ratio: 100:10:1). The total synthesis was completed within 34 min. The radioactivity of the final solution of [$^{11}$C]**1** was 3.4–5.4 GBq and the molar activity was 59–72 GBq/μmol ($n > 20$). The decay-corrected radiochemical yields based on [$^{11}$C]methyl iodide were 27–44%. The chemical and radiochemical purities were both >99%. The pH of the final solution was ≈7 (as measured using pH paper). These

qualities were considered to be fully applicable to in vivo animal PET study. HPLC chromatograms of the separation and the purity analyses of [$^{11}$C]**1** are shown in Supplementary Fig. 2.

### 2.6. PET imaging

PET imaging was performed as previously described with minor modifications.[20,24,25] We performed PET scanning 90 min after the fourth and tenth SDS. The experimental mice were anesthetized with 0.3–2.5% isoflurane and nitrous oxide/oxygen (7:3) and placed on the bed of a small-animal PET scanner (microPET Focus220, Siemens, Knoxville, TN, USA). A venous catheter for PET probe injection was inserted into the tail vein before PET scanning. $^{18}$F-labeled (*S*)-ketoprofen methyl ester or $^{11}$C-labeled probe [$^{11}$C]**1** (~20 MBq per animal) dissolved in 0.2 ml saline was injected via the cannula inserted into the tail vein for 10 s and emission data were then acquired either for 45 min ($^{18}$F-labeled (*S*)-ketoprofen methyl ester) or for 60 min ([$^{11}$C]**1**) using the 3D list-mode (6 × 10 s, 6 × 30 s, 11 × 60 s, and 15 × 180 s, for a total of 33 frames or 38 frames, respectively). The data were reconstructed with a standard 2D filtered back projection (ramp filter, cut-off frequency at 0.5 cycles per pixel). Regions of interest (ROIs) were placed on target organs using imaging processing software (PMOD ver. 4.0, PMOD Technologies, Fällanden, Switzerland) by aligning PET images to magnetic resonance T1-weighted images (Bruker BioSpec 70/20, Bruker Biospin MRI GmbH, Ettlingen, Germany) for the brain and computed tomography (CT) images (R-mCT2, Rigaku, Tokyo, Japan) for the other organs. For CT imaging, a contrast agent was injected via the cannula inserted into the tail vein. Regional uptake of radioactivity was expressed as the standardized uptake value (SUV), where SUV = tissue radioactivity concentration (MBq/cm$^3$)/[injected radioactivity (MBq)/body weight (g)]. Peak-normalized SUVs were calculated to account for the initial uptake of PET probes in target tissues, which may be influenced by stress-induced changes in blood flow. However, as the washout of PET probes may begin before the uptake is completed, unnormalized SUVs were also analyzed.

### 2.7. Quantitative RT-PCR

Quantitative RT-PCR was performed as previously described. Briefly, total RNA was extracted from tissues using TRIZOL Reagent (Thermo Fisher Scientific, Waltham, MA, USA) according to the manufacture's protocol. The resultant RNA was used to obtain cDNA using a PrimeScript RT reagent Kit with gDNA Eraser (Takara Bio, Shiga, Japan). All PCR experiments were conducted in duplicate using PowerTrack SYBR Green Master Mix (Thermo Fisher Scientific, Waltham, MA, USA), and fluorescent SYBR Green signals were automatically detected and analyzed with a CFX384 Touch Real-time PCR Detection System (Bio-Rad, Hercules, CA, USA). Primes for PCR are as follows: for mouse *Actb* (β-actin), 5′-TGC GTG ACA TCA AAG AGA AG-3′ and 5′-GAT GCCACA GGA TTC CAT A-3'; for mouse *Tlr4*, 5′-ATG GAA AAG CCT CGA ATC CT-3′ and 5′-TCC AAG TTG CCG TTT CTT GT-3'; for mouse *Tlr2*, 5′-TGG AAT GTC ACC AGG CTG C-3′ and 5′-GTC CGT GGA AAT GGT GGC-3'; for mouse *COX-1*, 5′-CCT CTT TCC AGG AGC TCA CA-3′ and 5'-TCG ATG TCA CCG TAC AGC TC-3'; for mouse *COX-2*, 5'-GGG AGT CTG GAA CAT TGT GAA-3′ and 5′-TGT CAA TCA AAT ATG ATC TGG ATG T-3'; for mouse *IL-1β*, 5'–AGT TGA CGG ACC CCA AAA G-3' and 5′-AGC TGG ATG CTC TCA TCA GG-3'; for mouse *IL-6*, 5′-GAG GAT ACC ACT CCC AAC AGA CC-3′ and 5′-AAG TGC ATC ATC GTT GTT CAT ACA-3'; for mouse Arg*1*, 5′-GGA ATC TGC ATG GGC AAC CTG TGT-3′ and 5′-AGG GTC TAC GTC TCG CAA GCC A-3'. The values were normalized to those of β-actin mRNA in the same cDNA samples. The levels were then normalized to those of the Control-Cerebellum groups.

### 2.8. Statistical analysis

Statistical analyses were performed using Prism 10 (GraphPad Software, San Diego, CA, USA). Error bars represent means ± SEM. Differences between two groups were analyzed with the two-tailed unpaired Student's *t*-test. Differences among more than two groups with two factors were analyzed with two-way ANOVA followed by Bonferroni's *post hoc* test for evaluation of pairwise group differences. *P*-values below 0.05 were considered statistically significant, unless specified otherwise in the text. Outliers were identified using the Robust regression and Outlier removal (ROUT) method.[26] This method identified one control mouse and one subchronic SDS mouse in TLR4 PET imaging as outliers and excluded them from the analysis. The number of samples in each group was determined based on published studies and our previous experience with the behavioral tests employed. No statistical methods were used to predetermine the sample size.

## 3. Results

### 3.1. Subchronic and chronic stress alters COX-1 PET activity in the kidneys and liver

To visualize the effects of stress on the distribution of COX-1 PET probes in the whole body, we subjected adult male C57BL/6N mice to chronic social defeat stress (SDS) (Fig. 1A). In this model, a single-housed male C57BL/6N mouse was exposed to aggressive encounters with a male ICR mouse for 10 min daily over 10 consecutive days. We first confirmed that chronic SDS increased the level of social avoidance, a typical stress-induced depression-related behavior (Fig. 1B and C). Since inflammation is a dynamic process composed of multiple phases, such as its initiation and resolution, we examined the distribution of COX-1 PET probes at two time points, after repeated SDS exposure four and ten times as subchronic and chronic stress, respectively (Fig. 1A). We used $^{18}$F-labeled *(S)*-ketoprofen methyl ester (*(S)*-[$^{18}$F]KTP-Me), a COX-1 PET probe that can be used to detect COX-1 distribution in mouse and human brains.[24,25,27] PET imaging was performed at 90 min after the last SDS exposure when SDS-induced inflammatory responses were clearly detected.[15] Regional uptake of radioactivity in each organ was expressed as the standardized uptake value (SUV), the radioactivity in a region of interest normalized to the whole-body concentration of the injected radioactivity. The summed SUVs of *(S)*-[$^{18}$F]KTP-Me showed a transient increase after subchronic SDS in the left kidney and a decrease only after chronic SDS in the liver (Supplementary Figs. 3A and B). The right kidney was excluded from the analysis due to potential contamination by liver signals.

In the kidney, the time activity curve of *(S)*-[$^{18}$F]KTP-Me showed two peaks within 1 min and 15 min, respectively (Supplementary Figs. 3C and D). This pattern is distinct from a washout of PET probes with exponential decay, suggesting that the radioactivity in the kidneys represents active biological processes, such as metabolism and excretion, that affect the accumulation of PET probes. Despite such complexity, subchronic SDS increased the first and second peaks in the left kidney (Supplementary Fig. 3C), whereas the second peak was rather decreased after chronic SDS (Supplementary Fig. 3D). These findings suggest stress-induced alteration in renal functions in a phase-dependent manner.

In the liver, the time activity curve showed a single peak, but the peak occurred more slowly, later than 1 min (Supplementary Figs. 3E and F), than in other tissues, such as the kidneys and brain. The washout was slower, with more than 50% of activity being persisted even after an hour (Supplementary Figs. 3E and F, right). This pattern is also distinct from a washout of PET probes with exponential decay, suggesting that the radioactivity in the liver also represents active biological processes. Chronic, but not subchronic, SDS reduced the uptake of COX-1 PET probes in the liver (Supplementary Fig. 3F, left), suggesting stress-induced alteration in liver functions.

Since the activity of COX-1 PET probes in the kidney and liver appears to be highly influenced by their pharmacokinetics, it is difficult to assess COX-1 expression in these organs with PET imaging.

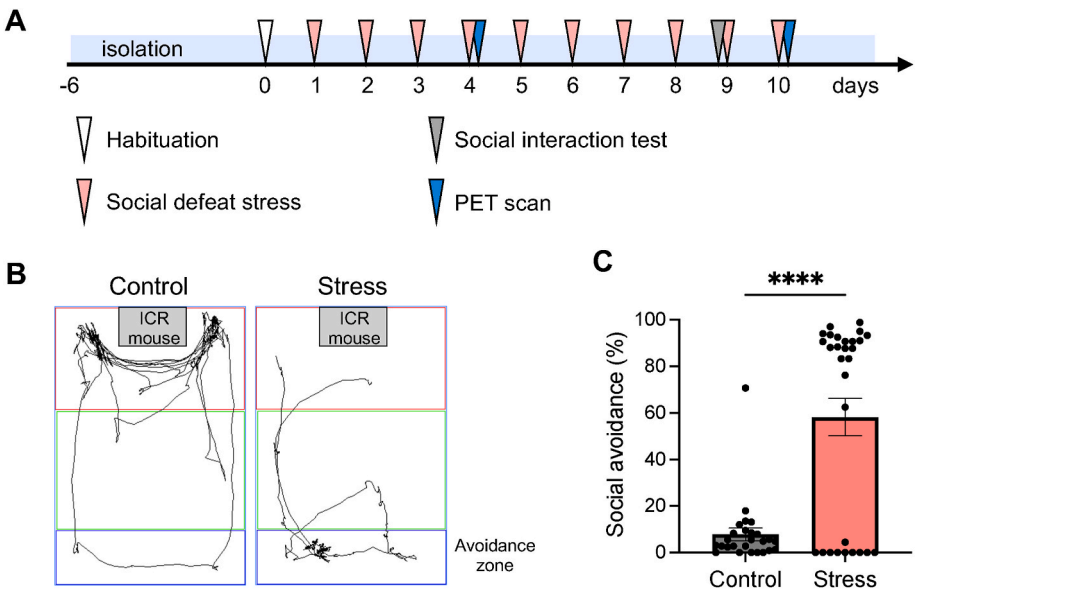


**Fig. 1.** Experimental schedule of PET imaging with mice after subchronic and chronic social defeat stress
(A) Experimental schedule of chronic SDS, social interaction test, and PET imaging. Mice were single-housed for 7 days, followed by habituation to the chamber used for the social interaction test on Day 0, one day before the first SDS. Then, mice were exposed to 10-min SDS per day over 10 consecutive days. PET imaging was performed 90 min after SDS on Day 4 and Day 10. The level of social avoidance was assessed by the social interaction test before SDS on Day 9.
(B) Definitions of the social avoidance zone (blue rectangles) and representative exploratory traces (black lines) of mice without or with chronic SDS (Control or Stress, respectively) in the social interaction test.
(C) The level of social avoidance in the social interaction test after chronic SDS. N = 26 for Control group, N = 29 for Stress group. ****$P < 0.0001$ for unpaired *t*-test. Error bars represent means ± SEM.

### 3.2. *Subchronic stress transiently alters COX-1 PET activity in the brain*

Since neuroinflammation is crucial for behavioral changes induced by chronic SDS,[14,15,17] we examined the distribution of the COX-1 PET probe *(S)*-[$^{18}$F]KTP-Me in the brain at 90 min after subchronic and chronic SDS. Subchronic SDS, but not chronic SDS, increased the summed SUV in the brain (Fig. 2A–C). The time activity curve showed rapid uptake within 1 min followed by rapid washout with exponential decay

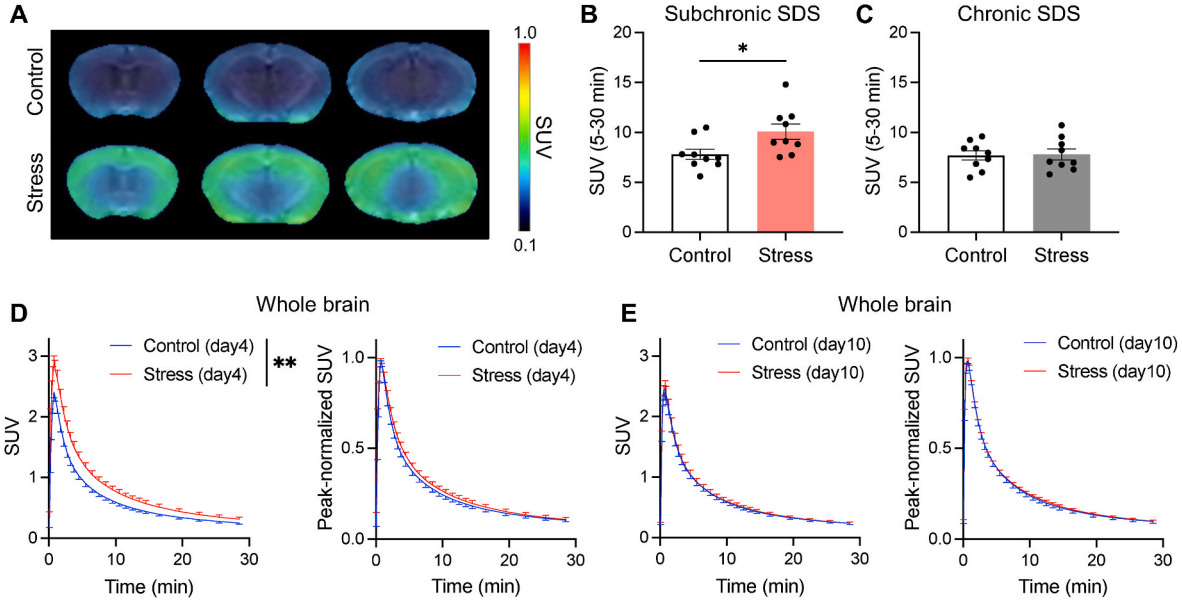


**Fig. 2.** Subchronic stress transiently alters COX-1 PET activity in the brain.
(A) Representative coronal views of PET images of *(S)*-[$^{18}$F]KTP-Me representing summed SUV from 5 to 45 min following probe injection at 90 min after subchronic SDS.
(B and C) The summed SUV of *(S)*-[$^{18}$F]KTP-Me from 5 to 30 min in the brain 90 min after subchronic (B) and chronic (C) SDS. N = 9 in each group. *$P < 0.05$ for unpaired *t*-test.
(D and E) The time activity curves of the SUV (left) and peak-normalized SUV (right) in the brain after subchronic (D, day 4) and chronic (E, day 10) SDS. The same PET images were analyzed as those in B and C. Blue and red lines represent Control and Stress (subchronic or chronic SDS) groups, respectively. **$P < 0.01$ for the main effect of stress in two-way repeated measures ANOVA.
Error bars represent means ± SEM.

(Fig. 2D and E). However, COX-1 PET activity in the brain persisted significantly longer than in the heart and lungs, with activity exceeding 67% in the brain compared to less than 34% in the heart and 42% in the lungs at 2 min post-injection (Supplementary Fig. 4). This observation suggests that the radioactivity at least partially represents COX-1 ligand binding in the brain, although the possibility of contamination from COX-1 PET activity in peripheral blood cannot fully be ruled out. Subchronic, but not chronic, SDS increased maximum uptake and slower washout of the probe in the brain (Fig. 2D), suggesting a transient increase of COX-1 ligand binding in the brain.

We then divided the whole brain into 10 regions and calculated the summed SUVs in each region (Fig. 3A and B). Subchronic, but not chronic, SDS increased the summed SUVs in most regions, especially the cerebral cortex, hippocampus, striatum, and thalamus, where the increase was statistically significant (Fig. 3A and B). The time activity curve showed rapid uptake within 1 min followed by rapid washout with exponential decay in all the brain regions examined (Fig. 3C–F). In subchronic SDS mice, the SUV was increased at the peak and remained elevated for at least 30 min in the cerebral cortex, hippocampus, striatum, and thalamus (Fig. 3C–F). The washout of COX-1 PET probes also appears to be slower even when the SUVs were normalized to the peak. These findings suggest that subchronic SDS transiently increased COX-1 ligand binding in these broad brain regions.

Notably, the peak-normalized time activity curve revealed the variability in the washout, which likely represents the different binding capacity of COX-1 PET probes, across brain regions in control and subchronic SDS mice (Fig. 3G and H). The delayed washout after subchronic SDS was most notable in the cerebral cortex and striatum and not related

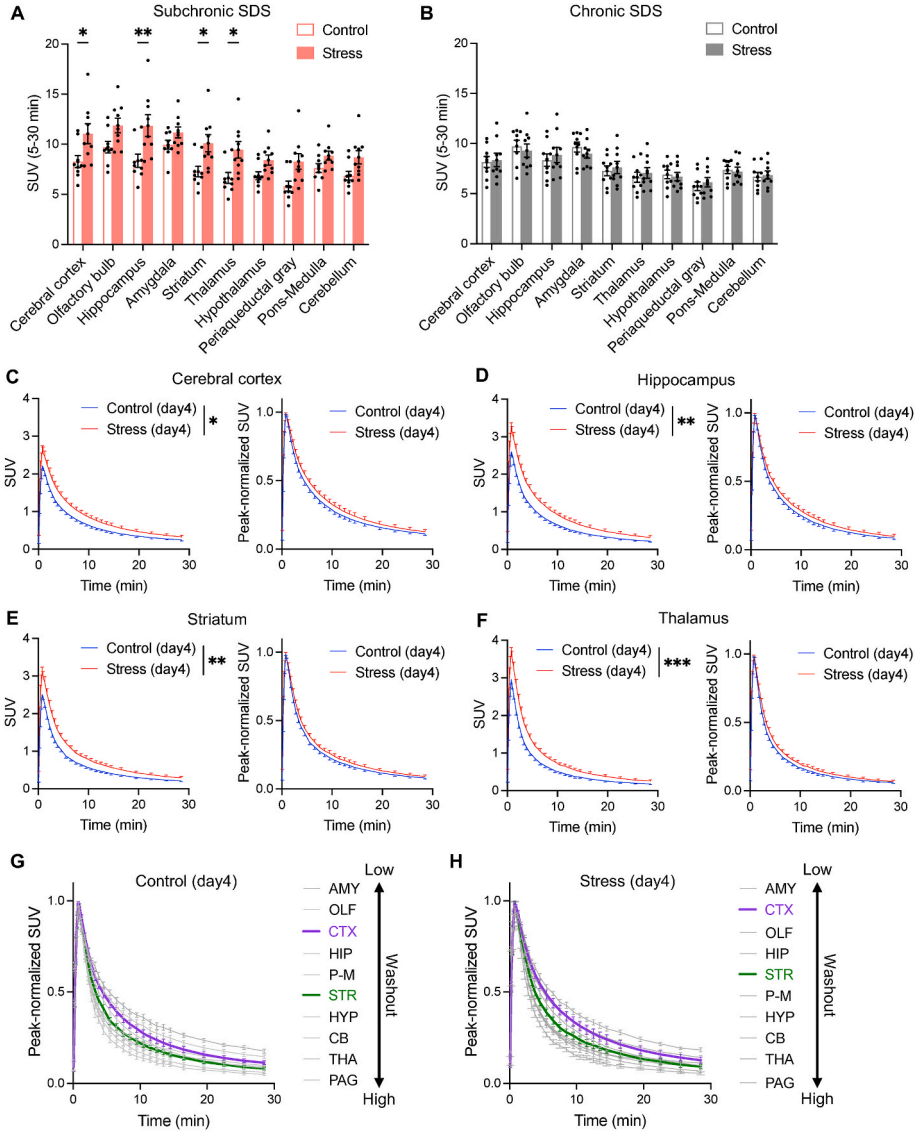


**Fig. 3.** Subchronic stress transiently alters COX-1 PET activity in the striatum, cerebral cortex, hippocampus, and thalamus.
(A and B) The summed SUV of *(S)*-[$^{18}$F]KTP-Me from 5 to 30 min in each brain region following probe injection at 90 min after subchronic (A) and chronic (B) SDS. N = 9 in each group. *$P < 0.05$, **$P < 0.01$ for Bonferroni's *post hoc* test after two-way ANOVA.
(C–F) The time activity curves of the SUV (left) and peak-normalized SUV (right) in the striatum (C), cerebral cortex (D), hippocampus (E), and thalamus (F) after subchronic SDS (day 4). The same PET images were analyzed as those in A and B. Blue and red lines represent Control and Stress groups, respectively. *$P < 0.05$, **$P < 0.01$, ***$P < 0.001$ for the main effect of stress in two-way repeated measures ANOVA.
(G and H) The time activity curves of the peak-normalized SUV in each brain region of control mice (G) and subchronic SDS mice (H). The washout decrease after subchronic SDS was most notable in the cerebral cortex and striatum (purple and green lines, respectively). AMY: amygdala, OLF: olfactory bulb, CTX: cerebral cortex, HIP: hippocampus, P–M: pons-medulla, STR: striatum, HYP: hypothalamus, CB: cerebellum, THA: thalamus, PAG: periaqueductal gray. N = 9 in each group. Error bars represent means ± SEM.

to the washout rate in control mice (Fig. 3H).

### 3.3. A novel PET probe for TLR4 detects inflammation in the brain

Given that the innate immune receptors TLR2/4 in microglia are crucial for behavioral disturbances induced by chronic SDS,[15] we developed a novel PET probe [$^{11}$C]**1** for TLR4, to visualize microglia-mediated neuroinflammation (Fig. 4A, see the Materials and Methods for details). To evaluate the effectiveness of [$^{11}$C]**1** in detecting inflammation in the brain, we unilaterally injected the TLR4 ligand lipopolysaccharide (LPS) into the striatum. The accumulation of [$^{11}$C]**1** at the injection site was compared to the corresponding site on the contralateral side. PET images taken one day after unilateral LPS injection into the striatum showed high accumulation of radioactivity on the injected striatum compared to the contralateral one (Fig. 4B, upper). Notably, a significant attenuation of [$^{11}$C]**1** accumulation by simultaneous injection of the non-radiolabeled **1** (1 mg/kg, approximately 500 folds chemical mass of [$^{11}$C]**1**) confirmed its specific binding in radioactivity (Fig. 4B and C). These results show that [$^{11}$C]**1** can effectively cross the blood-brain barrier and detect inflammation in the brain.

### 3.4. Subchronic and chronic stress alters TLR4 PET activity in the brain

We examined the distribution of the TLR4 PET probe [$^{11}$C]**1** in the brain at 90 min after subchronic and chronic SDS. The summed SUV in the whole brain did not show apparent effects of subchronic or chronic SDS (Fig. 5A–C). The time activity curve showed rapid peak within 1 min followed by rapid washout with exponential decay (Fig. 5D and E). TLR4 PET activity was distributed differently across brain regions, exhibited brain region-specific changes induced by SDS (see below for details), and distinctly from COX-1 PET activity. These observations suggest that the radioactivity of TLR4 PET probes at least partially represents their binding in the brain, although the possibility of contamination from TLR4 PET activity in peripheral blood cannot fully be ruled out. Subchronic and chronic SDS appears to increase the maximum uptake of the probe in the brain (Fig. 5D and E, left). However, when normalized to the peak, the washout of the probe was rather faster after subchronic and chronic SDS (Fig. 5D and E, right), suggesting a decrease of TLR4 ligand binding in the brain.

We then divided the whole brain into 10 regions and calculated the summed SUVs in each region (Fig. 6A and B). Since the uptake increase masks the effects of the washout increase in the summed SUVs, the peak-normalized, summed SUVs were also calculated (Fig. 6C and D). Indeed, the peak-normalized, summed SUVs showed clearer changes than the summed SUVs, such as the reduction in the cerebellum and pons-medulla (Fig. 6C and D). The time activity curve, especially when normalized to the peak, confirmed the faster washout in the cerebellum after subchronic and chronic SDS (Fig. 6E and F) and in the pons-medulla after chronic SDS (Fig. 6G and H), respectively. These findings suggest that subchronic and chronic SDS decreased TLR4 ligand

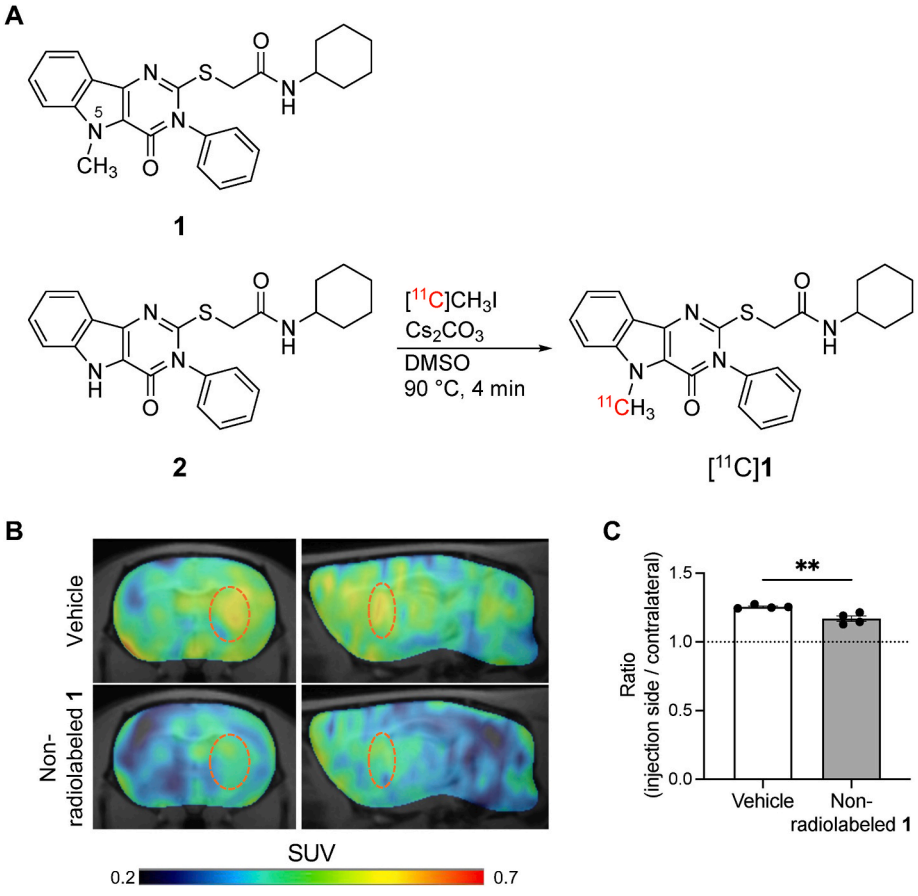


**Fig. 4.** A novel PET probe for TLR4 detects inflammation in the brain.
(A) Chemical structure and synthetic scheme of [$^{11}$C]**1**, a novel PET probe for TLR4.
(B) Representative coronal (left) and sagittal (right) views of [$^{11}$C]**1** PET images summed SUV from 5 to 45 min after probe injection without or with administration of non-radiolabeled compound (Vehicle or non-radiolabeled **1**, respectively) in rats microinjected LPS into the right striatum. Red ellipses indicate the sites of LPS injection.
(C) The ratio of the summed SUV from 5 to 45 min after probe injection in the region with LPS injection (red ellipses in A) and that in the corresponding contralateral region. N = 4 in each group. $^{**}P < 0.01$ for unpaired *t*-test.

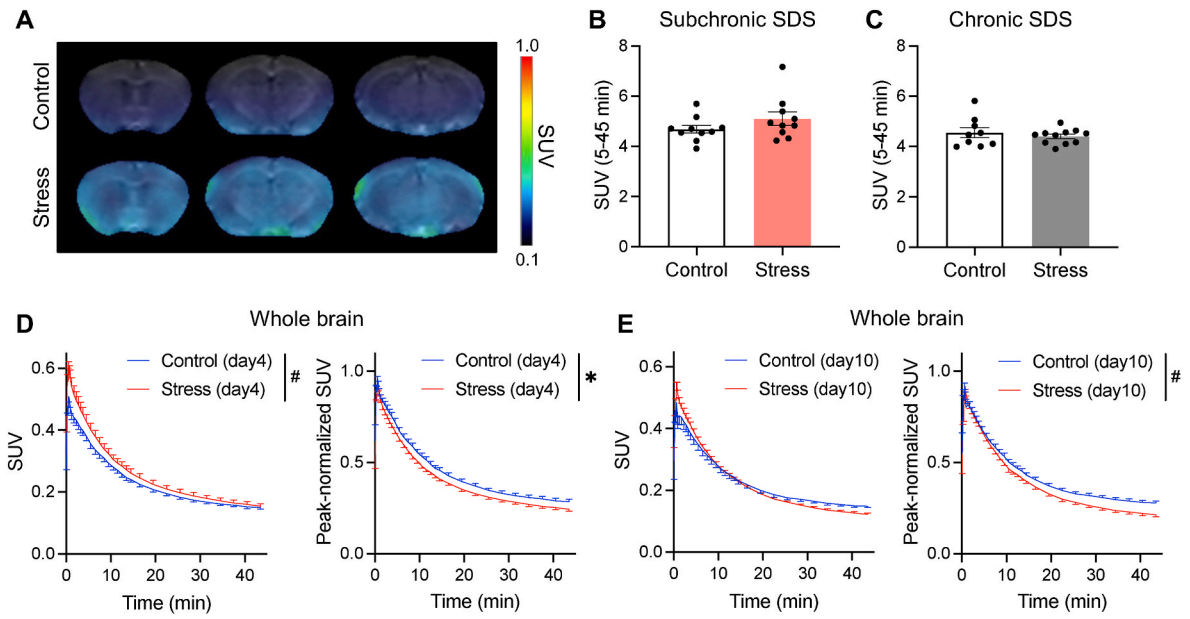


**Fig. 5.** Subchronic and chronic stress alters TLR4 PET activity in the brain.
(A) Representative coronal views of PET images of [$^{11}$C]**1** representing summed SUV from 5 to 45 min after probe injection following subchronic SDS.
(B and C) The summed SUV of [$^{11}$C]**1** from 5 to 45 min in the brain 90 min after subchronic (B) and chronic (C) SDS. N = 10 in each group in B, N = 9 for Control group and N = 11 for Stress group in C.
(D and E) The time activity curves of the SUV (left) and peak-normalized SUV (right) in the brain after subchronic (D, day 4) and chronic (E, day 10) SDS. The same PET images were analyzed as those in B and C. Blue and red lines represent Control and Stress groups, respectively. #$P < 0.1$, *$P < 0.05$ for the main effect of stress in two-way repeated measures ANOVA.
Error bars represent means ± SEM.

binding in these selective brain regions.

We examined TLR4 mRNA expression in the cerebellum and pons-medulla, where SDS accelerated the washout of TLR4 PET activity, as well as in the cerebral cortex, where it remained unaffected. We also examined COX-1 mRNA expression in these brain regions. Neither subchronic nor chronic SDS significantly altered TLR4 or COX-1 mRNA expression in any of these brain regions (Fig. 7A, B, H, and I), suggesting that their PET activities may reflect protein expression and/or other properties. Despite this, subchronic and chronic SDS did increase the mRNA expression of typical, if not all, inflammatory markers, such as COX-2 and IL-1β, in the cerebellum and pons-medulla (Fig. 7C–G and J-N), corroborating neuroinflammation implicated with TLR4 PET probes in these regions.

## 4. Discussion

Despite the roles of inflammation in mental illnesses, PET imaging with currently available markers has limitations due to the lack of evidence demonstrating their relationship to the molecular and cellular events of inflammation associated with mental illnesses. In this study, using the COX-1 PET probe *(S)*-[$^{18}$F]KTP-Me and a newly developed TLR4 PET probe, [$^{11}$C]**1**, we identified distinct alterations in COX-1 and TLR4 PET activity in the brain at multiple time points during chronic SDS. Thus, the increased uptake and slower washout of the COX-1 PET probe were transiently observed in widespread brain regions, such as the cerebral cortex, hippocampus, striatum, and thalamus, after subchronic SDS. By contrast, the washout of the TLR4 PET probe was rather increased in selective brain regions, the cerebellum after subchronic and chronic SDS and the pons-medulla after chronic SDS. Therefore, COX-1 and TLR4 PET imaging may be useful to visualize distinct molecular and cellular processes of neuroinflammation that drive stress-related mental illnesses.

PET imaging using TSPO ligands has been employed to visualize neuroinflammation, as increased TSPO expression in microglia and astrocytes is associated with neuroinflammation in various brain diseases. However, recent studies have shown that microglia and astrocytes play distinct roles in neuroinflammation and that microglia can exist in multiple states even within a single brain disease. Since TSPO is a general biomarker for all activated states of microglia and astrocytes, a molecular based, state-specific PET probe is needed to comprehensively investigate the specific pathophysiological role of neuroinflammation in brain diseases. In this study, PET imaging with COX-1 and TLR4 ligands in the brain revealed distinct spatiotemporal changes in their PET activity during chronic SDS: a transient, widespread change in COX-1 PET activity and a sustained, localized change in TLR4 PET activity. Given that COX-1 and TLR4 in microglia are critical for chronic SDS-induced behavioral disturbances, yet mediate different actions of microglia, PET imaging with COX-1 and TLR4 ligands may offer a novel approach to visualizing distinct neuroinflammatory states.

Since acute and chronic SDS increase COX-1-dependent $PGE_2$ synthesis selectively in subcortical rather than cortical regions,[14,17] COX-1 PET imaging does not accurately reflect the spatiotemporal pattern of COX-1-dependent $PGE_2$ synthesis. Neither subchronic nor chronic SDS affected COX-1 mRNA expression in the brain, suggesting that changes in COX-1 expression by PET reflect alterations in its protein expression, structure, and/or activity. Because COX-1 is selectively expressed in microglia and macrophages in the brain,[14] COX-1 expression detected by using PET may indicate a transient and widespread process of neuroinflammation during chronic stress. This finding contradicts the current notion, based on histological markers, that chronic stress induces microglial activation only in selective brain regions such as the medial prefrontal cortex (mPFC) and hippocampus.[15,28] Therefore, microglia and macrophages may exhibit widely distributed responses to chronic stress in the brain. Since changes in COX-1 expression detected by PET precede the development of chronic SDS-induced behavioral disturbances, COX-1 PET imaging might be useful for revealing neuroinflammation in the prodromal phase of mental illnesses.

Rodent studies have demonstrated that TLR2/4 in microglia underlie

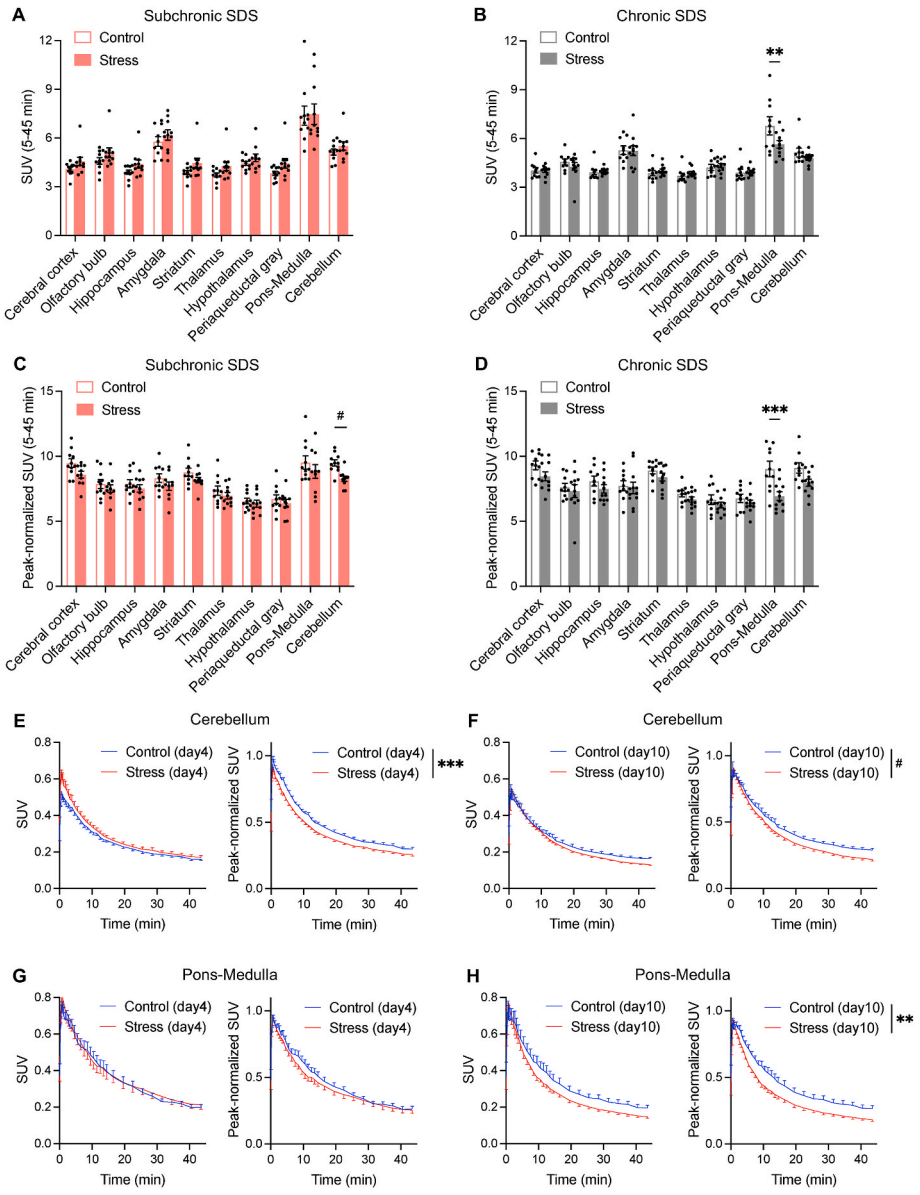


**Fig. 6.** Subchronic and chronic stress alters TLR4 PET activity in the cerebellum and brainstem.
(A–D) The summed SUV (A and B) and peak-normalized summed SUV (C and D) of [$^{11}$C]**1** from 5 to 30 min in each brain region 90 min following probe injection at 90 min after subchronic (A and C) and chronic (B and D) SDS. N = 10 in each group in A and C. N = 9 for Control group, N = 11 for Stress group in B and D. $\#P < 0.1$, $^{**}P < 0.01$, $^{***}P < 0.001$ for Bonferroni's *post hoc* test after two-way ANOVA.
(E–H) The time activity curves of the SUV (left) and peak-normalized SUV (right) in the cerebellum (E and F) and pons-medulla (G and H) after subchronic (E and G) and chronic (F and H) SDS. The same PET images were analyzed as those in A-D. Blue and red lines represent Control and Stress (subchronic or chronic SDS) groups, respectively. $\#P < 0.1$, $^{**}P < 0.01$, $^{***}P < 0.001$ for the main effect of stress in two-way repeated measures ANOVA.
Error bars represent means ± SEM.

multiple inflammatory processes in the brain, contributing to chronic stress-induced neuronal and behavioral disturbances.[15] Specifically, TLR2/4 mediate chronic stress-induced activation of mPFC microglia, leading to dendritic atrophy of mPFC neurons and behavioral disturbances through proinflammatory cytokines. Additionally, TLR2/4 play a crucial role in stress-induced $PGE_2$ synthesis in the microglia of the subcortical forebrain, which is responsible for the attenuation of the mPFC dopaminergic response and its behavioral consequences.[14,17] However, since peak-normalized TLR4 PET activity is selectively reduced in the cerebellum and pons-medulla, it does not reflect TLR2/4-dependent inflammatory processes in the forebrain and is distinct from the pattern of COX-1 PET activity.

Several possibilities may account for different results of COX-1 and TLR4 PET imaging. Since SDS did not alter the mRNA expression of COX-1 or TLR4, SDS-induced changes in COX-1 and TLR4 PET activity could reflect alterations in their protein expressions, structures, and/or activities. For example, microglia may proliferate, and macrophages may migrate to the site of neuroinflammation, thereby increasing the total amount of COX-1 protein in the tissue, hence binding to COX-1 PET probes. In addition, COX-1 is prone to suicidal inactivation with radicals derived from its enzymatic activity,[29] which may affect its protein expression, structure and activity. On the other hand, since TLR4 activation reportedly induces its endocytosis, reducing its surface expression,[30,31] the observed reduction in peak-normalized TLR4 PET activity could be attributed to alterations in its protein expression and/or localization. Thus, COX-1 and TLR4 expressions may vary differently depending on the states of microglia and the surrounding environment, which could influence their PET activity in distinct ways. TLR4 PET

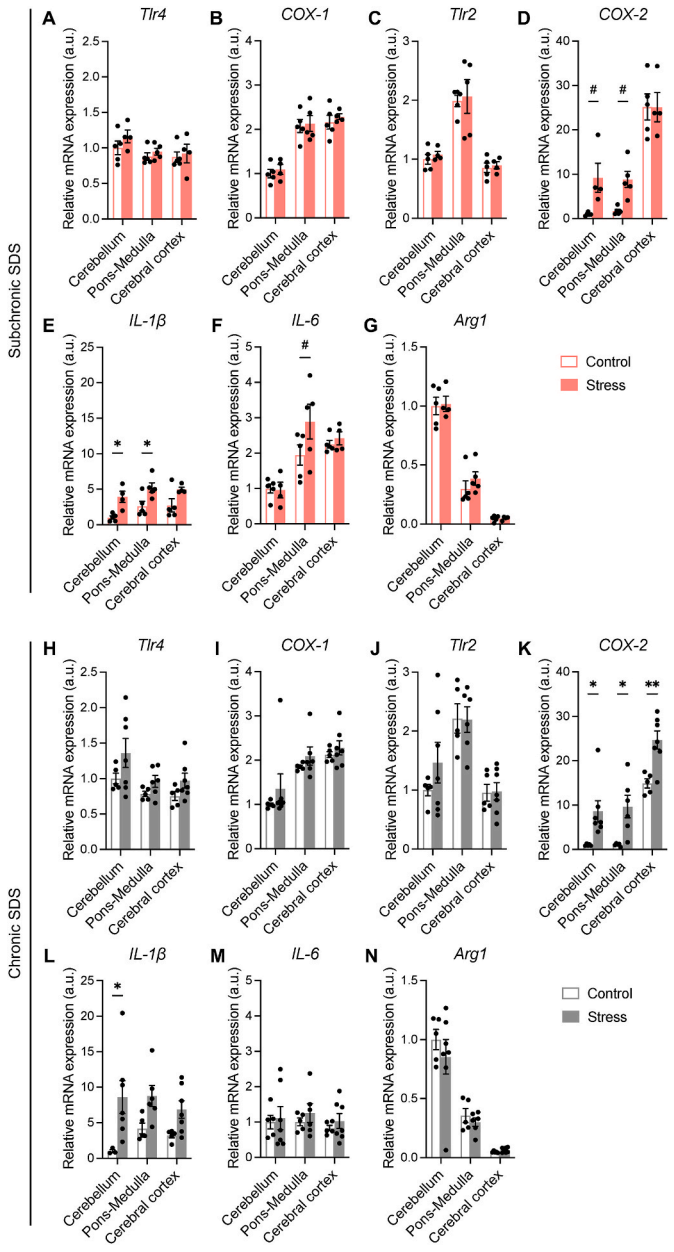


**Fig. 7.** Subchronic and chronic stress induces neuroinflammation in the cerebellum and brainstem. The relative mRNA expression levels of Tlr4 (A and H), COX-1 (B and I), Tlr2 (C and J), COX-2 (D and K), IL-1β (E and L), IL-6 (F and M), and Arg1 (G and N) in the cerebellum, pons-medulla, and cerebral cortex 90 min after subchronic (A–G) and chronic (H–N) SDS. #$P < 0.1$, *$P < 0.05$, **$P < 0.01$ for Bonferroni's *post hoc* test after two-way ANOVA. Error bars represent means ± SEM.

imaging may also reflect non-microglial changes during chronic SDS. Whereas COX-1 is selectively expressed in microglia, TLR4 is expressed not only in microglia but also in vascular endothelial cells,[32,33] whose barrier function is affected by chronic stress.[34] Therefore, the differential regulation and/or cell-type specificity of COX-1 and TLR4 expression may help explain the varying results observed with each PET probe.

Nonetheless, the pivotal role of TLR4 in inflammation suggests that TLR4 PET imaging can visualize unexpected neuroinflammatory processes localized in the cerebellum and pons-medulla, which are sustained during chronic SDS. Since subchronic and chronic SDS increased the expression of inflammatory markers, COX-2 and IL-1β, in the cerebellum and pons-medulla, neuroinflammation is likely to be induced in these regions. The pons-medulla contains serotonergic and noradrenergic neurons that have been implicated in chronic stress and depression.[35–37] Additionally, the cerebellum, particularly its non-motor regions, has been associated with depressive symptoms in clinical studies.[38–40] Rodent studies have also revealed the role of microglia in regulating monoaminergic and cerebellar neurons involved in emotional behavior.[41,42] Further investigation is needed to determine whether chronic stress-induced inflammation via TLR2/4 affects neuronal functions in the cerebellum and pons-medulla, contributing to behavioral disturbances.[29–31]

Consistent with the effects of chronic stress on bodily organs and their behavioral relevance,[3,7] subchronic and chronic SDS alter COX-1 PET activity in the kidneys and liver. However, since the activity does not follow a typical exponential decay due to the dissociation of the probe from its target, it may reflect SDS-induced changes in renal and hepatic functions. Indeed, chronic stress increases urine production,[43] a change that may be visualized by a subchronic SDS-induced increase in COX-1 PET activity in the kidneys. Additionally, chronic stress has been reported to affect the liver, which secretes inflammation-related molecules that infiltrate the brain parenchyma, leading to behavioral disturbances.[44,45] Thus, a chronic SDS-induced decrease in COX-1 PET activity in the liver may indicate hepatic dysfunction. Since the changes in COX-1 PET activity in the kidneys and liver appear to lack molecular specificity, another method is necessary to visualize the molecular processes underlying stress-induced renal and hepatic dysfunctions.

This study has several limitations. Whereas we developed TLR4 PET probes from a well characterized compound that selectively binds to TLR4 and validated their specificity in vivo using cold excess, their unknown metabolites produced in the body might exhibit unexpected off-target binding, which remains to be addressed with TLR4 knockout mice. Since COX-1 and TLR4 are abundantly expressed in peripheral blood cells, the potential contribution of these cells to brain PET activity remains to be excluded. In addition, PET imaging was conducted under anesthesia, which has been shown to affect microglial states through noradrenergic activity.[46,47] Therefore, to fully assess the applicability of these imaging modalities in humans, PET imaging of COX-1 and TLR4 should be performed in awake animals. It is also important to note that different animals were used for COX-1 and TLR4 PET imaging at different time points, and TSPO ligand imaging was not included in this study. Furthermore, as chronic SDS induces various behavioral changes, including depression, anxiety, and cognitive decline, the behavioral correlates of the PET imaging have yet to be examined. Given that specific neuronal circuits underlie such behavioral changes, the relationship between COX-1 and TLR4 expression and neuronal activity also warrants investigation. To address these issues and establish the unique advantages of COX-1 and TLR4 PET imaging for visualizing neuroinflammation, it is necessary to perform simultaneous COX-1 and TLR4 imaging, correlating the findings with behavioral disturbances at multiple time points during chronic SDS, and directly comparing them with FDG and TSPO PET imaging in the same subjects. Nonetheless, the specificity of COX-1 and TLR4 PET imaging in the brain, likely due to molecular and cellular precision, cannot be achieved with currently available markers of neuroinflammation, such as TSPO ligands. These novel imaging tools may be used to identify and analyze multiple neuroinflammatory processes with distinct spatiotemporal patterns in human patients with stress-related mental illnesses, such as depression and PTSD.

## CRediT authorship contribution statement

**Yumika Motooka:** Investigation. **Ryota Shinohara:** Writing – review & editing, Writing – original draft, Supervision, Investigation, Funding acquisition, Conceptualization. **Shiho Kitaoka:** Investigation, Conceptualization. **Ai Uryu:** Investigation. **Dongrui Li:** Investigation. **Hiroyuki Neyama:** Investigation. **Yilong Cui:** Writing – review & editing, Methodology, Investigation, Conceptualization. **Tatsuya Kida:** Methodology. **Wakiko Arakaki:** Methodology. **Hisashi Doi:** Writing –

review & editing, Methodology. **Yasuyoshi Watanabe:** Writing – review & editing, Supervision, Methodology, Funding acquisition, Conceptualization. **Tomoyuki Furuyashiki:** Writing – review & editing, Writing – original draft, Supervision, Funding acquisition, Conceptualization.

## Funding

This study was supported by grants from AMED (JP17gm0910012, JP24wm0425001, JP24zf0127010, and JP24zf0127012 to T.F., JP24gm6310028 to R.S., JP17gm0910012 to Y.W.), Grants-in-Aid for Scientific Research from the Ministry of Education, Culture, Sports, Science and Technology in Japan (JP21H04812 and JP24K22086 to T.F., JP22K06859 to R.S.), JST Moonshot R&D (JPMJMS239F to T.F.).

## Competing interests

The authors have no competing interests to disclose.

## Acknowledgments

We thank Misako Takizawa (Kobe University) for secretarial help and Yuta Ochi and Yuuki Tamura (RIKEN) for technical help. We also thank Emi Hayashinaka (RIKEN) for operating PET scanners.

## Appendix A. Supplementary data

Supplementary data to this article can be found online at https://doi.org/10.1016/j.jphs.2025.01.006.

## References

1. Lupien SJ, McEwen BS, Gunnar MR, Heim C. Effects of stress throughout the lifespan on the brain, behaviour and cognition. *Nat Rev Neurosci.* 2009;10(6):434–445. https://doi.org/10.1038/nrn2639.
2. Sanacora G, Yan Z, Popoli M. The stressed synapse 2.0: pathophysiological mechanisms in stress-related neuropsychiatric disorders. *Nat Rev Neurosci.* 2022;23(2):86–103. https://doi.org/10.1038/s41583-021-00540-x.
3. Ishikawa Y, Furuyashiki T. The impact of stress on immune systems and its relevance to mental illness. *Neurosci Res.* 2022;175:16–24. https://doi.org/10.1016/j.neures.2021.09.005.
4. Cathomas F, Holt LM, Parise EM, et al. Beyond the neuron: role of non-neuronal cells in stress disorders. *Neuron.* 2022;110(7):1116–1138. https://doi.org/10.1016/j.neuron.2022.01.033.
5. Iwata M, Ota KT, Duman RS. The inflammasome: pathways linking psychological stress, depression, and systemic illnesses. *Brain Behav Immun.* 2013;31:105–114. https://doi.org/10.1016/j.bbi.2012.12.008.
6. Furman D, Campisi J, Verdin E, et al. Chronic inflammation in the etiology of disease across the life span. *Nat Med.* 2019;25(12):1822–1832. https://doi.org/10.1038/s41591-019-0675-0.
7. Chan KL, Poller WC, Swirski FK, Russo SJ. Central regulation of stress-evoked peripheral immune responses. *Nat Rev Neurosci.* 2023;24(10):591–604. https://doi.org/10.1038/s41583-023-00729-2.
8. Dowlati Y, Herrmann N, Swardfager W, et al. A meta-analysis of cytokines in major depression. *Biol Psychiatry.* 2010;67(5):446–457. https://doi.org/10.1016/j.biopsych.2009.09.033.
9. Setiawan E, Wilson AA, Mizrahi R, et al. Role of translocator protein density, a marker of neuroinflammation, in the brain during major depressive episodes. *JAMA Psychiatr.* 2015;72(3):268–275. https://doi.org/10.1001/jamapsychiatry.2014.2427.
10. Setiawan E, Attwells S, Wilson AA, et al. Association of translocator protein total distribution volume with duration of untreated major depressive disorder: a cross-sectional study. *Lancet Psychiatr.* 2018;5(4):339–347. https://doi.org/10.1016/s2215-0366(18)30048-8.
11. Holmes SE, Hinz R, Conen S, et al. Elevated translocator protein in anterior cingulate in major depression and a role for inflammation in suicidal thinking: a positron emission tomography study. *Biol Psychiatry.* 2018;83(1):61–69. https://doi.org/10.1016/j.biopsych.2017.08.005.
12. Guilarte TR, Rodichkin AN, McGlothan JL, Rocha AMADL, Azzam DJ. Imaging neuroinflammation with TSPO: a new perspective on the cellular sources and subcellular localization. *Pharmacol Ther.* 2022;234, 108048. https://doi.org/10.1016/j.pharmthera.2021.108048.
13. Nutma E, Fancy N, Weinert M, et al. Translocator protein is a marker of activated microglia in rodent models but not human neurodegenerative diseases. *Nat Commun.* 2023;14(1):5247. https://doi.org/10.1038/s41467-023-40937-z.
14. Tanaka K, Furuyashiki T, Kitaoka S, et al. Prostaglandin E2-mediated attenuation of mesocortical dopaminergic pathway is critical for susceptibility to repeated social defeat stress in mice. *J Neurosci.* 2012;32:4319–4329. https://doi.org/10.1523/jneurosci.5952-11.2012.
15. Nie X, Kitaoka S, Tanaka K, et al. The innate immune receptors TLR2/4 mediate repeated social defeat stress-induced social avoidance through prefrontal microglial activation. *Neuron.* 2018;99:464–479. https://doi.org/10.1016/j.neuron.2018.06.035. e7.
16. Narumiya S. Physiology and pathophysiology of prostanoid receptors. *Proc Jpn Acad Ser B Phys Biol Sci.* 2007;83(9-10):296–319. https://doi.org/10.2183/pjab/83.296.
17. Nie X, Kitaoka S, Shinohara M, Kakizuka A, Narumiya S, Furuyashiki T. Roles of Toll-like receptor 2/4, monoacylglycerol lipase, and cyclooxygenase in social defeat stress-induced prostaglandin E2 synthesis in the brain and their behavioral relevance. *Sci Rep.* 2019;9(1), 17548. https://doi.org/10.1038/s41598-019-54082-5.
18. Shimizu T. Lipid mediators in Health and disease: enzymes and receptors as therapeutic targets for the regulation of immunity and inflammation. *Annu Rev Pharmacol Toxicol.* 2009;49(1):123–150. https://doi.org/10.1146/annurev.pharmtox.011008.145616.
19. Iwasaki A, Medzhitov R. Regulation of adaptive immunity by the innate immune system. *Science.* 2010;327(5963):291–295. https://doi.org/10.1126/science.1183021.
20. Shukuri M, Mawatari A, Takatani S, et al. Synthesis and preclinical evaluation of $^{18}$F-labeled ketoprofen methyl esters for cyclooxygenase-1 imaging in neuroinflammation. *J Nucl Med.* 2022;63(11):1761–1767. https://doi.org/10.2967/jnumed.121.263713.
21. Shinohara R, Taniguchi M, Ehrlich AT, et al. Dopamine D1 receptor subtype mediates acute stress-induced dendritic growth in excitatory neurons of the medial prefrontal cortex and contributes to suppression of stress susceptibility in mice. *Mol Psychiatry.* 2018;23:1717–1730. https://doi.org/10.1038/mp.2017.177.
22. Chan M, Hayashi T, Mathewson RD, et al. Identification of substituted pyrimido[5,4-*b*]indoles as selective toll-like receptor 4 ligands. *J Med Chem.* 2013;56(11):4206–4223. https://doi.org/10.1021/jm301694x.
23. Chan M, Kakitsubata Y, Hayashi T, et al. Structure–activity relationship studies of pyrimido[5,4-*b*]indoles as selective toll-like receptor 4 ligands. *J Med Chem.* 2017;60(22):9142–9161. https://doi.org/10.1021/acs.jmedchem.7b00797.
24. Shukuri M, Takashima-Hirano M, Tokuda K, et al. In vivo expression of cyclooxygenase-1 in activated microglia and macrophages during neuroinflammation visualized by PET with $^{11}$C-ketoprofen methyl ester. *J Nucl Med.* 2011;52(7):1094–1101. https://doi.org/10.2967/jnumed.110.084046.
25. Shukuri M, Mawatari A, Ohno M, et al. Detection of cyclooxygenase-1 in activated microglia during amyloid plaque progression: PET studies in alzheimer's disease model mice. *J Nucl Med.* 2016;57(2):291–296. https://doi.org/10.2967/jnumed.115.166116.
26. Motulsky HJ, Brown RE. Detecting outliers when fitting data with nonlinear regression – a new method based on robust nonlinear regression and the false discovery rate. *BMC Bioinform.* 2006;7(1):123. https://doi.org/10.1186/1471-2105-7-123.
27. Ohnishi A, Senda M, Yamane T, et al. Exploratory human PET study of the effectiveness of 11C-ketoprofen methyl ester, a potential biomarker of neuroinflammatory processes in Alzheimer's disease. *Nucl Med Biol.* 2016;43(7):438–444. https://doi.org/10.1016/j.nucmedbio.2016.04.005.
28. Iwata M, Ota KT, Li XY, et al. Psychological stress activates the inflammasome via release of adenosine triphosphate and stimulation of the purinergic type 2X7 receptor. *Biol Psychiatry.* 2016;80(1):12–22. https://doi.org/10.1016/j.biopsych.2015.11.026.
29. Song I, Ball TM, Smith WL. Different suicide inactivation processes for the peroxidase and cyclooxygenase activities of prostaglandin endoperoxide H synthase-1. *Biochem Biophys Res Commun.* 2001;289(4):869–875. https://doi.org/10.1006/bbrc.2001.6071.
30. Tanimura N, Saitoh S, Matsumoto F, Akashi-Takamura S, Miyake K. Roles for LPS-dependent interaction and relocation of TLR4 and TRAM in TRIF-signaling. *Biochem Biophys Res Commun.* 2008;368(1):94–99. https://doi.org/10.1016/j.bbrc.2008.01.061.
31. Kagan JC, Su T, Horng T, Chow A, Akira S, Medzhitov R. TRAM couples endocytosis of Toll-like receptor 4 to the induction of interferon-β. *Nat Immunol.* 2008;9(4):361–368. https://doi.org/10.1038/ni1569.
32. Johnson RH, Kho DT, Carroll SJO, Angel CE, Graham ES. The functional and inflammatory response of brain endothelial cells to Toll-Like Receptor agonists. *Sci Rep.* 2018;8(1), 10102. https://doi.org/10.1038/s41598-018-28518-3.
33. Tsioti I, Steiner BL, Escher P, Zinkernagel MS, Benz PM, Kokona D. Endothelial Toll-like receptor 4 is required for microglia activation in the murine retina after systemic lipopolysaccharide exposure. *J Neuroinflammation.* 2023;20(1):25. https://doi.org/10.1186/s12974-023-02712-1.
34. Menard C, Pfau ML, Hodes GE, et al. Social stress induces neurovascular pathology promoting depression. *Nat Neurosci.* 2017;20(12):1752–1760. https://doi.org/10.1038/s41593-017-0010-3.
35. Zou WJ, Song YL, Wu MY, et al. A discrete serotonergic circuit regulates vulnerability to social stress. *Nat Commun.* 2020;11(1):4218. https://doi.org/10.1038/s41467-020-18010-w.
36. Isingrini E, Perret L, Rainer Q, et al. Resilience to chronic stress is mediated by noradrenergic regulation of dopamine neurons. *Nat Neurosci.* 2016;19:560–563. https://doi.org/10.1038/nn.4245.
37. Ruhé HG, Mason NS, Schene AH. Mood is indirectly related to serotonin, norepinephrine and dopamine levels in humans: a meta-analysis of monoamine

depletion studies. *Mol Psychiatry*. 2007;12(4):331–359. https://doi.org/10.1038/sj.mp.4001949.
38. Peng J, Liu J, Nie B, et al. Cerebral and cerebellar gray matter reduction in first-episode patients with major depressive disorder: a voxel-based morphometry study. *Eur J Radiol*. 2011;80(2):395–399. https://doi.org/10.1016/j.ejrad.2010.04.006.
39. Liu L, Zeng LL, Li Y, et al. Altered cerebellar functional connectivity with intrinsic connectivity networks in adults with major depressive disorder. *PLoS One*. 2012;7(6), e39516. https://doi.org/10.1371/journal.pone.0039516.
40. Depping MS, Schmitgen MM, Kubera KM, Wolf RC. Cerebellar contributions to major depression. *Front Psychiatry*. 2018;9:634. https://doi.org/10.3389/fpsyt.2018.00634.
41. Yamamoto M, Kim M, Imai H, Itakura Y, Ohtsuki G. Microglia-triggered plasticity of intrinsic excitability modulates psychomotor behaviors in acute cerebellar inflammation. *Cell Rep*. 2019;28(11):2923–2938.e8. https://doi.org/10.1016/j.celrep.2019.07.078.
42. Takahashi A, Aleyasin H, Stavarache MA, et al. Neuromodulatory effect of interleukin 1β in the dorsal raphe nucleus on individual differences in aggression. *Mol Psychiatry*. 2022;27(5):2563–2579. https://doi.org/10.1038/s41380-021-01110-4.
43. Shimizu T, Shimizu S, Higashi Y, Saito M. Psychological/mental stress-induced effects on urinary function: possible brain molecules related to psychological/mental stress-induced effects on urinary function. *Int J Urol*. 2021;28(11):1093–1104. https://doi.org/10.1111/iju.14663.
44. Mondal A, Bose D, Saha P, et al. Lipocalin 2 induces neuroinflammation and blood-brain barrier dysfunction through liver-brain axis in murine model of nonalcoholic steatohepatitis. *J Neuroinflammation*. 2020;17(1):201. https://doi.org/10.1186/s12974-020-01876-4.
45. Yan L, Yang F, Wang Y, et al. Stress increases hepatic release of lipocalin 2 which contributes to anxiety-like behavior in mice. *Nat Commun*. 2024;15(1):3034. https://doi.org/10.1038/s41467-024-47266-9.
46. Cao K, Qiu L, Lu X, et al. Microglia modulate general anesthesia through P2Y12 receptor. *Curr Biol*. 2023;33(11):2187–2200.e6. https://doi.org/10.1016/j.cub.2023.04.047.
47. Haruwaka K, Ying Y, Liang Y, et al. Microglia enhance post-anesthesia neuronal activity by shielding inhibitory synapses. *Nat Neurosci*. 2024;27(3):449–461. https://doi.org/10.1038/s41593-023-01537-8.